



HAL
open science

Impact of a pressurized membrane: Coefficient of restitution

Baptiste Darbois Texier, Loïc Tadrast

► **To cite this version:**

Baptiste Darbois Texier, Loïc Tadrast. Impact of a pressurized membrane: Coefficient of restitution. Physical Review E , 2023, 107 (5), pp.055001. 10.1103/PhysRevE.107.055001 . hal-04089454

HAL Id: hal-04089454

<https://hal.science/hal-04089454>

Submitted on 4 May 2023

HAL is a multi-disciplinary open access archive for the deposit and dissemination of scientific research documents, whether they are published or not. The documents may come from teaching and research institutions in France or abroad, or from public or private research centers.

L'archive ouverte pluridisciplinaire **HAL**, est destinée au dépôt et à la diffusion de documents scientifiques de niveau recherche, publiés ou non, émanant des établissements d'enseignement et de recherche français ou étrangers, des laboratoires publics ou privés.

Impact of a pressurised membrane: coefficient of restitution

Baptiste Darbois Texier

*Université Paris-Saclay, CNRS, FAST, 91405, Orsay, France.**

Loïc Tadrist[†]

*Aix-Marseille Université, CNRS, ISM, Marseille, France**

(Dated: today)

Pressurised membranes are usually used for low cost structures (e.g. inflatable bed), impact protections (e.g. air-bags) or sport balls. The last two examples deal with impacts on human body. Under-inflated protective membranes are not effective whereas over-inflated objects can cause injury **at impact**. The coefficient of restitution represents the ability of a membrane to dissipate energy during an impact. Its dependence on membrane properties and inflation pressure is investigated on a model experiment using a spherical membrane. Coefficient of restitution increases with inflation pressure but decreases with impact speed. For a spherical membrane, it is shown that kinetic energy is lost by transfer to vibration modes. A physical modelling of a spherical membrane impact is build considering a quasi-static impact with small indentation. Finally, the dependency of the coefficient of restitution with mechanical parameters, pressurisation and impact characteristics is given.

I. INTRODUCTION

Pressurised elastic shells are ubiquitous, whether as natural or artificial systems. The latter case includes airbags [1], inflated helmets [2], inflated shoes [3, 4], airbag suits [5], inflatable structures [6, 7] and sport balls [8]. The inflation pressure allows to adjust the mechanical properties of these systems, as an increase in pressure increases the rigidity of the shell. The fact that the mechanical properties of these systems can be easily changed makes them suitable for the interaction with humans and in particular for protection against impacts.

The mechanical response of pressurised shells has been investigated in the limit of quasi-static deformations. A pressurised spherical shell indented locally has been shown to experience a wrinkling instability above a critical indentation [9]. This observation was rationalised by considering that the overpressure introduces an effective bending stiffness in the system that competes with the natural bending stiffness of the shell. The wrinkling pattern that develops above the instability threshold was latter captured by a linear stability analysis of the problem [10].

The limit of rapid deformations has been extensively studied in the case of a pressurised membrane impacting a rigid substrate [11]. In this situation, the contact dynamics between the pressurised shell and the substrate can be characterised by a coefficient of restitution. This quantity corresponds to the ratio between the ingoing speed and the outgoing speed $\eta = |U_{\text{out}}/U_0|$. The coefficient of restitution reflects the loss of kinetic energy during the impact. η is unity for lossless impacts. However, the simplicity of the definition of the coefficient of restitution masks the multiple possible physical origins

of energy loss for a pressurised membrane. A fraction of the membrane kinetic energy may be transferred to (i) membrane vibrations [12], (ii) the ambient media vibrations (sound [13] and ground vibrations); heat converted by (iv) viscous dissipation in the membrane, (v) friction with the ground, or (vi) thermally exchanged during impact (non-adiabatic compression-expansion cycle of the internal gas). Deciphering between those physical origins of energy dissipation will shape a theory to predict the evolution of coefficient of restitution with inflation pressure, membrane mechanical parameters and impact speed.

Specifically for spherical shells, two different physical explanations have been proposed to account for the loss of energy during the impact of a pressurised membrane, the momentum flux force [8] and the visco-elastic dissipation within the membrane [14]. The momentum flux force theory does not specify the physical phenomena responsible for energy loss. It stands that the work of the force corresponding to the non-linear acceleration of the membrane during the compression phase is not restored during the expansion phase. In a different manner, viscoelastic dissipation corresponds to heat production within the membrane material. This dissipation has been modelled with a linear damping force proportional to indentation velocity [14]. This empirical model did not link explicitly the damping coefficient to the mechanical parameters of the pressurised membrane.

In this paper, we investigate the dependence of the coefficient of restitution with the mechanical properties of the pressurised membrane. We chose to study a thin spherical membrane made of elastomer and inflated with air as a model system. We first present two sets of measurements of coefficient of restitution by systematically varying impact speed and inflation pressure for a small and a large membrane. Second, we observe the part of the pressurised membrane in contact with the ground during the impact and rule out losses by friction. Then, we compare the different predictions of the coefficient of

* loic.tadrist@univ-amu.fr

[†] <http://ism-cbi.duckdns.org>

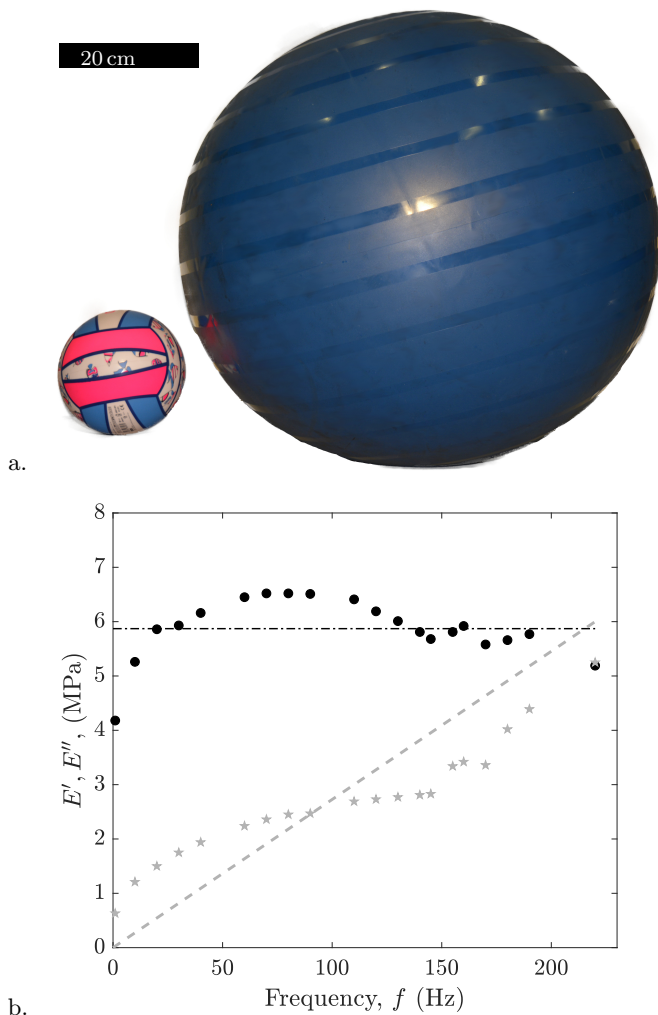


FIG. 1. a. Small ball and large ball considered as models of pressurised membranes in this paper. b. Mechanical properties of the elastomer of membranes (BV100 fun) as a function of forcing frequency with an elongation of 1% and preload of 0.1%. (\bullet): E' and (\star): E'' . Grey dashed line slope corresponds to $2\pi\mu = 27$ kPa.s.

restitution and show that vibrations of the membrane are the main sources of energy losses. This is rationalised combining idealised kinematics of ball impact [15] and a minimal 1-mode vibration modelling. Finally, the dependence of the coefficient of restitution with pressure, impact speed and membrane mechanical parameters is established.

II. IMPACTS OF PRESSURISED MEMBRANES : EXPERIMENTS

A. Characteristics of the pressurised membranes

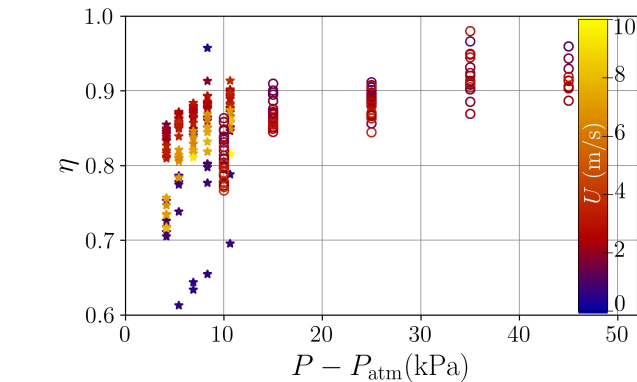
For spherical membranes, we used a set of four small beach-volley balls (BV100 fun, Decathlon KIPSTA) of

deflated radius was $R = 8.2 \pm 0.1$ cm, and one large gym ball (gym ball size 3, Decathlon DOMYOS) of deflated radius $R = 31.3 \pm 0.4$ cm (see figure 1a). Those spherical membranes were chosen for their minimal composition: they consist of a single layer of elastomer with a valve for inflation. We set the inflation pressure $P - P_{\text{atm}}$ where P is the absolute inner pressure in the membrane and P_{atm} is the atmospheric pressure. The small membrane weighed $m = 179$ g and the large membrane weighed $m = 2.6$ kg. Both membranes had a thickness $e = 2.00 \pm 0.12$ mm. We verified that the mass of the membrane corresponds to $m = 4\pi\rho R^2 e$ with ρ the density of the elastomeric material constituting the membrane.

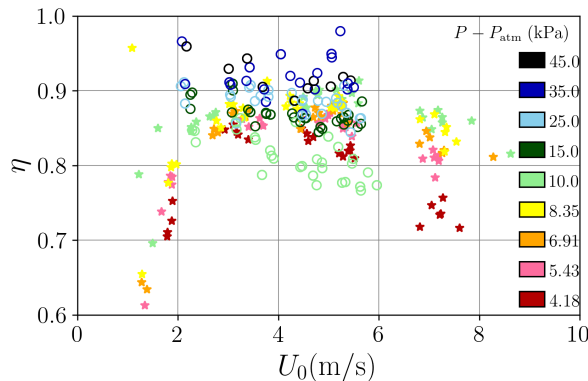
Membrane elastomer was isotropic and was characterised with a dynamical viscometer to determine the storage modulus E' and loss modulus E'' . The pieces of elastomer tested on the viscometer were rectangles of width 9.0 ± 0.1 mm and length 20.6 ± 0.1 mm. They were clamped on their width and the test temperature was 25°C . Over the range of tested frequencies, E' was almost constant $E' \simeq 5.9 \pm 1.0$ MPa and E'' varied linearly with frequency leading to $E''/f = 2\pi\mu \simeq 27 \pm 3$ kPa.s, see figure 1b, where μ is the effective viscosity of the material. The Young modulus of the membrane at rest (i.e. $f = 0$ Hz) was $E = 4.2 \pm 0.1$ MPa. The loss modulus was measured on non pre-stretched samples of elastomer, see figure 1b. However, when the membrane is inflated, the elastomer is necessarily pre-stretched. In our conditions, the pre-stretching of the membrane has been estimated to be smaller than 20% [15] and is expected to slightly decrease the loss modulus E'' [16].

B. Coefficient of restitution as a function of inflation pressure and impact speed

We report here measurements of the impact properties of the pressurised membranes varying impact speed U_0 and inflation pressure $P - P_{\text{atm}}$. Experimental data of coefficient of restitution for small membranes impacts were already reported in a previous publication [15] but data regarding the large gym ball are original. For both series of measurements, we followed the same protocol where the ball was dropped from a height h on a rigid substrate and a high speed camera allowed to determine the ingoing and outgoing speeds of the ball, providing an estimate for $\eta = |U_{\text{out}}/U_0|$. A home-made Matlab code detected the circular shape of the membrane. It provided the position of the circle in time filtering out deformations and vibrations of the membrane. The coefficient of restitution η is plotted in figure 2a (respectively figure 2b) as a function of the inflation pressure $P - P_{\text{atm}}$ (respectively impact speed U_0). In the range of low speeds ($U_0 < 2$ m s $^{-1}$), the coefficient of restitution increases with the impact speed whereas for larger impact speeds $U_0 > 2$ m s $^{-1}$ it decreases. In the following, we focus on impact speeds larger than 2 m s $^{-1}$. In this range, the coefficient of restitution increases slightly with

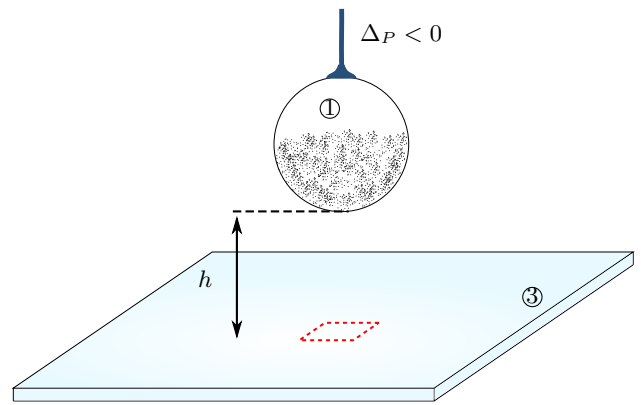


a.

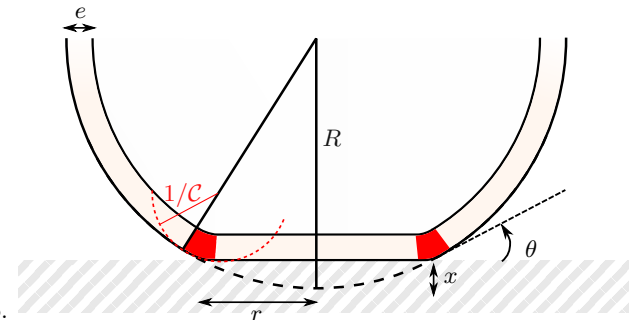


b.

FIG. 2. a. Coefficient of restitution η as a function of inflation pressure $P - P_{\text{atm}}$. Open symbols: small membrane. Filled symbol: large membrane. Colors give information about impact velocity. b. Coefficient of restitution η as a function of impact velocity U_0 . Open symbols: small membrane. Filled symbol: large membrane. Colors give information about inflation pressure.



a.



b.

FIG. 3. a. Schematics of the experiment to image membrane displacements at the contact. The pressurised membrane is released from a height h . ① Spherical membrane painted with synthetic Schlieren. ② Imaging facility. ③ clear window for imaging from below. b. Parametrisation of membrane during contact.

150 inflation pressure but decreases with impact speed.

151 C. Deformations at the contact

152 Tests of membrane deformations kinematics were car- 168
 153 ried out on small membranes (BV100 Fun) using a stereo- 169
 154 imaging digital image correlation set-up (DIC standard 170
 155 3D, *Dantec dynamics*), see figure 3a. The membrane was 171
 156 inflated at recommended pressure $P - P_{\text{atm}} = 15 \text{ kPa}$. 172
 157 It was then prepared for image correlation: first the 173
 158 ball surface was gently sanded using fine-grained sand- 174
 159 paper to remove superficial paint. The clean white mem- 175
 160 brane was then finely sprayed black to create a synthetic 176
 161 Schlieren for image correlation. 177

162 The set-up consisted of a suction device to release the 178
 163 ball without initial velocity nor spin from a height h . 179
 164 Suction was produced thanks to a commercial vacuum 180
 165 cleaner. A large glass plate was used as transparent sub- 181

strate. Lighting and imaging at 300 Hz were done from 166
 167 below. Stereo imaging was performed with two cameras 168
 with a slight angle (6°) regarding the vertical.

Image correlation is performed during contact with the 169
 170 glass plate. Figure 4a shows that the pressurised mem- 171
 172 brane is flattened on the ground without crumpling, dif- 173
 174 ferently as suggested in the case of basket balls [13]. The 174
 175 deformations show a radial compression of the flattened 175
 176 part of the membrane. The magnitude of the radial com- 176
 177 pression increases with radial distance.

Figure 4b shows the difference between an impact im- 178
 179 age and the image at the time of largest indentation. The 179
 180 difference shows a black spot at the contact location indi- 180
 181 cating that no or negligible slip occurs during the contact 181
 of the membrane with the glass plate. If buckling had oc- 181
 curred, this would have create a white spot at the center

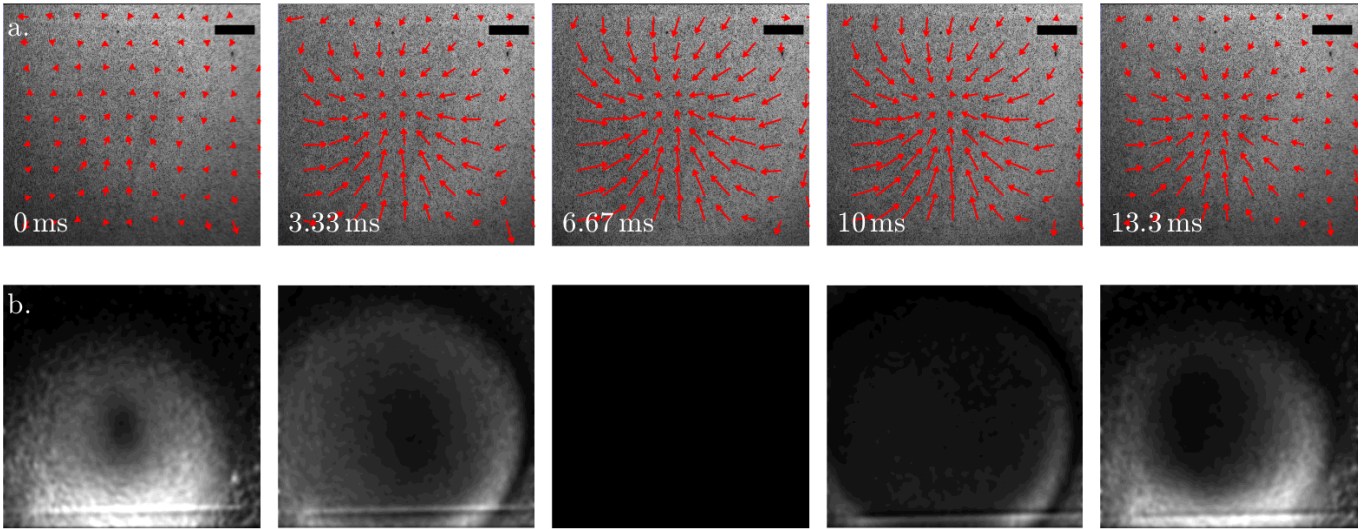


FIG. 4. Contact kinematics of the membrane. a. Contact area between the ball and the glass plate seen from below at different times after the impact at $t = 0$ ms. Red arrows (not scaled) indicate the compression displacement field computed by digital image correlation. b. Difference between current image and maximal indentation image at 6.67 ms. Scale bar is 1 cm.

182 of the images in figure 4b. One would also notice ar-212
 183 rows pointing towards the ring of the fold (with reversal-213
 184 inside the ring) which is not the case, see red arrows fig-214
 185 ure 4a. Differently to the contact of rigid spherical shells-215
 186 where buckling occurs [17, 18] and involves solid friction,-216
 187 the contact of a pressurised membrane involves neither
 188 buckling nor friction in the range of impact conditions
 189 explored here.

190 This difference could result from the fact that internal
 191 pressure prevents the buckling transition. The effect of-217
 192 the internal pressure on the onset of wrinkling of an elas-218
 193 tic membrane submitted to a point load has been studied-219
 194 by Vella *et al.* [9]. In the limit of high pressure, they-220
 195 showed that wrinkles appear above a critical indentation-221
 196 x_c ,
 222
 223

$$\frac{x_c}{R} = 2.52 \frac{(P - P_{\text{atm}})R}{Ee}. \quad (1)$$

197 Considering typical experimental values used here, $P -$ 224
 198 $P_{\text{atm}} = 15$ kPa, $R = 8$ cm, $e = 2$ mm, $E = 4$ MPa, the
 199 criterion given by Eq. (1) yields $x_c/R \simeq 0.38$. In the
 200 range of impact speeds and pressurisation explored in
 201 this study, the maximal indentation experienced by the
 202 pressurised membrane is $x_{\text{max}}/R < 0.20$, and the pre-225
 203 vious criteria is never reached. This explains why no
 204 buckling nor wrinkling is observed for sufficiently pres-
 205 surised membranes in contrast with previous observa-
 206 tions made on shells [17]. A scaling similar to that of
 207 Eq. (1) arises when considering mirror buckling of the-227
 208 membrane. Pauchard and Rica analysed mirror buckling-228
 209 by comparing non-buckled (I) and buckled (II) energies
 210 of non-pressurised shells indented on a flat surface. In the
 211 non-buckled state, indentation creates bending in the fold

(flat-to-spherical junction) and stretching in the flat sec-
 tion. Differently, when buckled, only bending in the fold
 is present but with a larger angle. For a non-pressurised
 shell, energies of states I and II depend on indentation
 depth x , see figure 3b, and read,

$$E_{\text{I}} = \frac{C_0}{4} \frac{Ee^{5/2}}{R} x^{3/2} + C_1 \frac{Ee}{R} x^3 \quad \text{and} \quad E_{\text{II}} = C_0 \frac{Ee^{5/2}}{R} x^{3/2} \quad (2)$$

where C_0 and C_1 are numerical constants. In order to
 account for pressurisation in this approach, we consider
 the adiabatic gas compression into the energy balance
 (no thermal exchange). In state I, gas volume is reduced
 by the one of the spherical cap approximated by $\pi R x^2$,
 whereas, it is reduced by twice this volume in state II
 and Eqs. (2) transform as,

$$E_{\text{I}} = \frac{C_0}{4} \frac{Ee^{5/2}}{R} x^{3/2} + C_1 \frac{Ee}{R} x^3 + \pi R (P - P_{\text{atm}}) x^2 \quad (3)$$

and

$$E_{\text{II}} = C_0 \frac{Ee^{5/2}}{R} x^{3/2} + 2\pi R (P - P_{\text{atm}}) x^2 \quad (4)$$

Buckling is expected when $E_{\text{I}} > E_{\text{II}}$ which leads to a
 non-linear equation with 3 terms,

$$\frac{3C_0}{4} \frac{Ee^{5/2}}{R} x^{3/2} + \pi R (P - P_{\text{atm}}) x^2 - C_1 \frac{Ee}{R} x^3 = 0 \quad (5)$$

In the case of pressurised membranes with $C_0 \simeq 0$, the
 buckling criterion reads,

$$\frac{x_c}{R} = \frac{\pi(P - P_{\text{atm}})R}{C_1 E e}. \quad (6)$$

This approach gives a similar scaling as the one proposed in [9] and suggests that this result does not depend crucially on the geometry of the deformed area. Thus, the conclusion drawn above should be valid for spherical membranes indenting a flat surface, considering a different prefactor.

III. COEFFICIENT OF RESTITUTION OF A PRESSURISED MEMBRANE

The coefficient of restitution corresponds to a loss of kinetic energy during the impact. This energy may be lost in different manners, either from viscous dissipation in the membrane (in the curved fold or in the stretched flat part), or by transfer to mechanical vibrations of the membrane. The other physical phenomena involved during the impact (sound emission [13], thermal exchange through the membrane [15] and friction/buckling, see above) are much less energetic.

A. Predictions of dissipated power

1. Dissipated power by stretching

During the impact, a fraction of the membrane changes its shape from a spherical shell to a flat surface of radius r (see figure 3b). In order to adapt to this change, the membrane must stretch. As the material constituting the membrane is visco-elastic, this deformation induces a loss of energy. In order to estimate this dissipation, we look at the deformation of the membrane during the impact in the region of the fold. Locally, the membrane forms an angle θ with the ground which respects $\sin \theta = r/R$. At this location, a small portion of the spherical part of length ℓ has to compress by a length $\Delta \ell = \ell(\cos \theta - 1)$ to become flat. Thus, the membrane experiences a deformation $\varepsilon_s = \Delta \ell / \ell = \cos \theta - 1$. In the limit of small indentations ($x \ll R$), corresponding to $\theta \ll 1$, the membrane deformation becomes $\varepsilon_s \simeq -\theta^2/2$ and the angle reduces to $\theta \simeq r/R$. The viscous energy associated to a deformation occurring in a volume dV is $dE_{\text{strech}} = \mu \varepsilon_s \dot{\varepsilon}_s dV$. Considering a portion of the membrane located in the interval r and $r + dr$, the deformation affects a material volume $2\pi r e dr$ and we get the following expression for the power dissipated by stretching,

$$\frac{dE_{\text{strech}}}{dt} = \pi \mu e \frac{r^4 \dot{r}^2}{R^4}. \quad (7)$$

In the limit of small indentations ($x \ll R$), the radius of contact is related to the indentation of the spherical membrane by $r^2 \simeq 2Rx$ (see figure 3b) and equation (7) becomes,

$$\frac{dE_{\text{strech}}}{dt} = 2\pi \mu e \frac{x \dot{x}^2}{R} \quad (8)$$

2. Dissipated power by bending in the fold

The flat part of the membrane is connected to the spherical part of the membrane by a fold. The characteristic size of the fold δ is fixed by a competition between bending and stretching energies as described in [17], leading to $\delta \simeq \sqrt{eR}$. The fold volume is $V_{\text{fold}} = 2\pi r e \delta \simeq 2\pi R \sqrt{2x e^3}$ since the contact radius is $r \simeq \sqrt{2Rx}$ when $x \ll R$. The radius of curvature of the fold scales as $1/C \sim \delta/\theta$, where $\theta \simeq \sqrt{2x/R}$ is the contact angle of the membrane, see figure 3b. The bending deformations in the fold scale as $\varepsilon_b \sim e C \sim \sqrt{2x e}/R$ during the typical deformation time $\tau \sim \delta/\dot{r} \sim \sqrt{2x e}/\dot{x}$ that corresponds to the fold dimension divided by the fold velocity. The viscous stresses are thus $\sigma \sim \mu \varepsilon_b / \tau$ where μ is the equivalent viscosity of the membrane. Finally, the dissipated power in the fold scales as,

$$\frac{dE_{\text{fold}}}{dt} \sim \mu \frac{\varepsilon_b^2}{\tau^2} V_{\text{fold}} \sim \mu \frac{e^{3/2} \sqrt{x} \dot{x}^2}{R}. \quad (9)$$

3. Dissipated energy by vibrations

Vibrations of the membrane can be described by the vibration modes of a pressurised spherical shell by decomposition of the deformed membrane on spherical harmonics as realised by Feshbach et al. [19, p1469]. To simplify the description of vibrations, we consider a minimal model of two masses connected by a spring, see figure 5a. This model was first developed to describe the rebound of a water droplet impacting a hydrophobic surface [20]. In this model, the first mass, mass 1 located in x_1 , corresponds to the mass of membrane that will not contact the ground whereas the other mass, mass 2 located in x_2 , corresponds to the amount of membrane that will contact the ground at the maximal indentation of the impact. The two masses m_1 and m_2 are connected by a linear spring of rigidity k and rest length l_0 , see figure 5a. Before contact, both masses move with a velocity U_0 towards the ground. When mass 2 makes contact with the ground, it stops ($U_2 = 0$) and mass 1 compresses the spring. The contact ends when the spring recovers its rest length l_0 . At this moment mass 2 still has no velocity. We assume that no dissipation occurs in the system, which implies that the total kinetic energy is preserved and mass 1 takes off with velocity $U_1 = \sqrt{1 + m_2/m_1} U_0$. The difference in speed between masses 1 and 2 creates vibrations. The vibration energy reads

$$E_{\text{vib}} = \frac{1}{2} m_2 U_0^2, \quad (10)$$

where m_2 is the fraction of the membrane of volume $2\pi R e x_{\text{max}}$ in contact with the ground at maximum indentation and which expresses as

$$m_2 = \frac{m x_{\text{max}}}{2R} = \frac{1}{2} \sqrt{\frac{m^3 U_0^2}{\pi R^3 (P - P_{\text{atm}})}}, \quad (11)$$

as the maximal indentation of the membrane expresses
 $x_{\max} = U_0 \sqrt{m/\pi R(P - P_{\text{atm}})}$ when the dissipation term
 is neglected [15]. The total energy transferred to vibrations
 according the two-mass model is

$$E_{\text{vib}} = \frac{1}{4} \frac{(mU_0^2)^{3/2}}{\sqrt{\pi R^3(P - P_{\text{atm}})}}. \quad (12)$$

This energy is ultimately be dissipated as heat in the material.

B. Coefficient of restitution in the limit of small dissipation

In this section, we examine the implications of the previous energy dissipation scenarios on the coefficient of restitution. For the sake of simplicity, we assume that the membrane dynamics is not affected by the dissipation. This approximation is motivated by the fact that the pressurised membrane is equivalent to a damped oscillator system with a quality factor larger than 10 ($\eta > 0.7$). In these conditions, the dissipation shifts the natural frequency of the system by less than one percent in relative value. Under these circumstances, the behaviour of the pressurised membrane at impact is linear and indentation evolves as [15],

$$x(t) = \sqrt{\frac{mU_0^2}{\pi R(P - P_{\text{atm}})}} \sin\left(\sqrt{\frac{\pi R(P - P_{\text{atm}})}{m}} t\right), \quad (13)$$

In this limit, one can compute the dissipated energy in the membrane from Eqs. (8) and (9)

$$E_{\text{stretch}} = \frac{2\pi\mu e}{R} \int_0^{t_c} \dot{x}^2 x dt = \frac{4\mu e m U_0^3}{3R^2(P - P_{\text{atm}})}, \quad (14)$$

$$E_{\text{fold}} = \frac{\mu e^{3/2}}{R} \int_0^{t_c} \dot{x}^2 \sqrt{x} dt = 1.61 \frac{\mu U_0^{5/2} e^{3/2} m^{3/4}}{(P - P_{\text{atm}})^{3/4} R^{7/4}}, \quad (15)$$

with $t_c = \pi \times \sqrt{m/(\pi R(P - P_{\text{atm}}))}$. Under these conditions, we derive three predictions for the coefficient of restitution associated with the different origins of dissipation:

$$\eta_{\text{stretch}} = \sqrt{1 - \frac{2E_{\text{stretch}}}{mU_0^2}} \simeq 1 - \frac{4\mu e U_0}{3R^2(P - P_{\text{atm}})}, \quad (16)$$

$$\eta_{\text{fold}} = \sqrt{1 - \frac{2E_{\text{fold}}}{mU_0^2}} \simeq 1 - 1.61 \frac{\mu U_0^{1/2} e^{3/2}}{m^{1/4}(P - P_{\text{atm}})^{3/4} R^{7/4}}, \quad (17)$$

$$\eta_{\text{vib}} = \sqrt{1 - \frac{2E_{\text{vib}}}{mU_0^2}} \simeq 1 - \frac{\sqrt{mU_0^2}}{4\sqrt{\pi R^3(P - P_{\text{atm}})}}. \quad (18)$$

These three predictions for the coefficient of restitution have different dependencies with the mechanical parameters of the pressurised membrane. Thus, one can hope to distinguish between the three scenarios for energy dissipation by comparing these predictions to experiments. Figure 5b presents the parity plot between the predicted coefficient of restitution η_{model} from Eqs. (16), (17) and (18) as a function of the measured coefficient of restitution η_{exp} for small and large membranes, different inflation pressures and impact speeds. In this representation, experiments match theoretical predictions when data points align on the $y = x$ line (dashed line). We observe that both viscoelastic dissipation models fail in gathering data points showing that this physical background of energy dissipation is unlikely. However predictions of the energy dissipated in the two-mass model gather all data points on a line $\eta_{\text{model}} - 1 = 0.63(\eta_{\text{exp}} - 1)$ (dotted line). This suggests that the scaling given for energy dissipation is correct although missing the prefactor on mass 2. This conclusion is reinforced by the fact that the agreement is valid over a wide range of parameters: the size of the membrane has been varied by a factor 4, the impacting speed by a factor 8 and the inflation pressure by a factor 9.

IV. DISCUSSION

The fact that the pressurised membrane dissipates the energy into vibrations has several consequences which are discussed in this section. First, the energy dissipated does not depend on the loss modulus μ of the elastomer constituting the membrane (see Eq. (18)). Thus, the viscoelastic dissipative properties of the membrane does not affect its bouncing quality. Second, Eq. (18) predicts that the coefficient of restitution decreases linearly with U_0 and with $1/\sqrt{P - P_{\text{atm}}}$. This allows to rationalise the decrease of η with U_0 and its increase with $P - P_{\text{atm}}$ observed experimentally for impact speeds $U_0 > 2 \text{ m s}^{-1}$.

The expression for the coefficient of restitution given by Eq.(18) relies on several assumptions. First, the pressurised membrane is modelled by two masses connected by a linear spring, an hypothesis that is valid only at small indentations. For large indentations, the non-linear elastic behaviour of the pressurised membrane due to gas compression has to be considered. This effect, described in [15], corresponds to a strain-stiffening behavior, it reduces both contact time and maximal indentation. Compared to the prediction of the linear model, the membrane is expected to be less deformed and thus to dissipate less energy. Second, we assume that the impact dynamics of the pressurised membrane is only marginally modified by the dissipation at small indentations. At larger indentations, energy dissipation would have to be taken into account in the impact dynamics and would modify Eq. (13). Accounting for dissipation in the impact dynamics would increase the contact time.

In the present modelling, we assumed that the

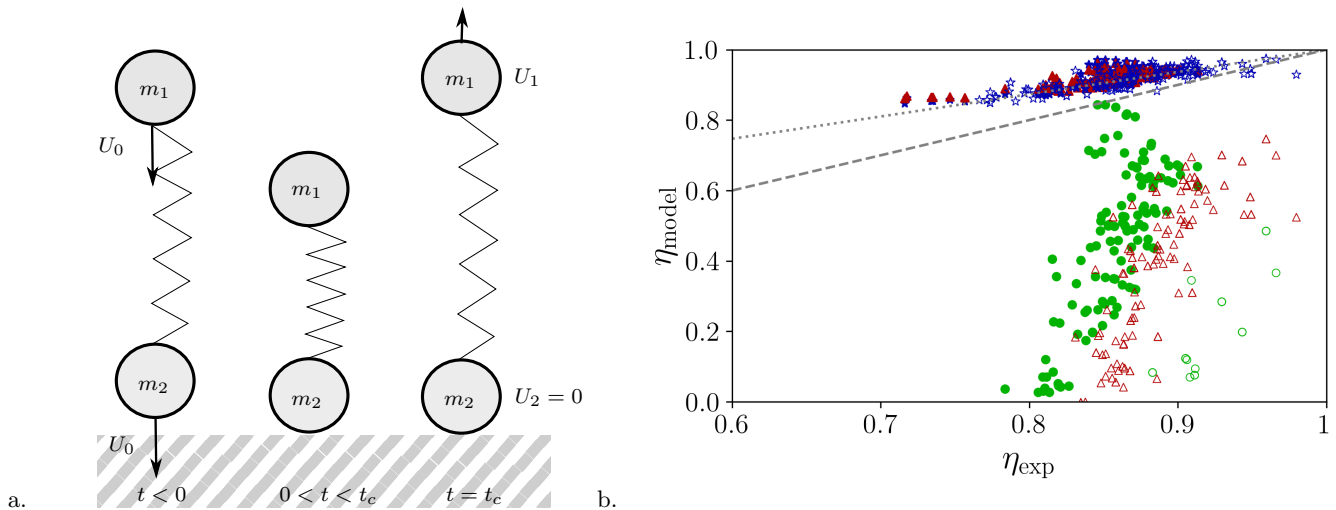


FIG. 5. a. Toy model of the 2-mass system. b. Parity plot of Eqs. (16) in green, (17) in red and (18) in blue. Open symbols correspond to the small membrane and filled symbols correspond to the large membrane. Dashed line: parity $\eta_{\text{model}} = \eta_{\text{exp}}$. Dotted line: fit $1 - \eta_{\text{model}} = 0.63(1 - \eta_{\text{exp}})$

inflation-induced pre-stretching of the membrane was constant and that all results were derived linearly around this reference state. When indentation of the membrane is large, the linear mechanics hypothesis breaks down. The impact becomes non-linear because of both large displacements with geometrical stiffening and non-linear material behaviour such as strain-stiffening or strain-softening. The geometrical stiffening would reduce the amount of deformed material and decrease dissipation.

The knowledge of the origin of the dissipation in the impact is interesting for practical situations where low or high coefficients of restitution may be required. For impact protection applications, a low coefficient of restitution helps to reduce the amount of momentum exchanged during the impact. When a pressurised membrane of mass m impacts onto a massive ground, the change of momentum of the membrane is $2mU_0$ in a perfectly elastic case, twice the exchange of momentum that occurs during a perfectly inelastic impact mU_0 . For sport balls, a minimal coefficient or restitution is prescribed by the rules in order to insure that the ball can be released with sufficient speed. In sports, a maximal inner pressure is also prescribed (which corresponds to a maximal coefficient of restitution for a given impact speed). This may be related to the decrease of contact time as the inner pressure increases. This change of contact time increases the rate of exchange of momentum (i.e. impact inertial forces) and thus the severity of impact-related damages. It also reduces the possibility for the player to control the ball trajectory during contact.

This study considers the origin of dissipation when a pressurised membrane impacts a rigid ground. The coefficient of restitution of small and large inflated membranes has been measured for a wide range of internal

pressures and impact speeds. Four possible sources of energy dissipation in this problem have been considered. Solid friction has been discarded by performing image visualisation in the contact area. The other possible sources of dissipation are the compression of the flattened membrane, the bending of the visco-elastic membrane in the fold and the energy transferred to vibrations. A physical prediction for each dissipation scenario has been computed and compared to measurements. The deformation of the pressurised membrane during the impact was considered through the framework of linear mechanics around the reference state of the pressurised shell. Impact-induced deformations are mainly the consequence of the impact kinematics.

Based on experimental data, we concluded that during the impact of a pressurised membrane with a rigid ground, **the energy is dissipated in vibrations and this may be predicted by a two-mass model**. Identifying the source of dissipation in this problem should help in improving the design of impact protections and a better understanding of the role of ball inflation pressure in sport. This work opens multiple perspectives as improving the modelling of membrane vibrations beyond the simple model of two masses connected by a linear spring, characterising the membrane vibrations after impact which is challenging from a technical point-of-view and considering the effect of the impactor geometry on the dissipation that takes place during impact.

ACKNOWLEDGEMENT

The authors thank Stéphane Méo and Marie-Pierre Defargues for their welcome at CERMEL lab and use of the traction bench. The authors thank Laurent Aprin

- 481 and Tristan Gilet for the loan of high-speed cameras. Au-486
 482 thors thank Tristan Gilet, Christophe Clanet, Caroline487
 483 Cohen, Lounès Tadrist, François Lanzetta, Aisha Med-488
 484 ina, Jean-Marc Linares, Santiago Arroyave-Tobón, Julien489
 485 Chaves-Jacob and Ludovic Pauchard for valuable help
-
- 490 [1] H. Zhou, Z. Zhong, M. Hu, Design and occupant-523
 491 protection performance analysis of a new tubular driver524
 492 airbag, *Engineering* 4 (2018) 291–297. 525
- 493 [2] M. Kurt, K. Laksari, C. Kuo, G. A. Grant, D. B. Ca-526
 494 marillo, Modeling and optimization of airbag helmets for527
 495 preventing head injuries in bicycling, *Annals of biomed-528*
 496 ical engineering 45 (2017) 1148–1160. 529
- 497 [3] N. Mills, Running shoe materials, *Materials in sports530*
 498 equipment 1 (2003) 65. 531
- 499 [4] K. Baousi, N. Fear, C. Mourouzis, B. Stokes, H. Wood,532
 500 P. Worgan, A. Roudaut, Inflashoe: A shape changing533
 501 shoe to control underfoot pressure, in: *Proceedings of534*
 502 the 2017 CHI Conference extended abstracts on humans535
 503 factors in computing systems, 2017, pp. 2381–2387. 536
- 504 [5] B. Nemeth, M. van der Kaaij, R. Nelissen, J.-K. van Wi-537
 505 jnen, K. Drost, G. J. Blauw, Prevention of hip fractures538
 506 in older adults residing in long-term care facilities with539
 507 a hip airbag: a retrospective pilot study, *BMC geriatrics540*
 508 22 (2022) 1–7. 541
- 509 [6] J. Krauel, N. Ferguson, *Inflatable: Art, Architecture &542*
 510 *Design*, Links, 2013. 543
- 511 [7] R. B. Malla, T. G. Gionet, Dynamic response of a pres-544
 512 surized frame-membrane lunar structure with regolith545
 513 cover subjected to impact load, *Journal of Aerospace546*
 514 *Engineering* 26 (2013) 855–873. 547
- 515 [8] W. Stronge, A. Ashcroft, Oblique impact of inflated balls548
 516 at large deflections, *International journal of impact en-549*
 517 gineering 34 (2007) 1003–1019. 550
- 518 [9] D. Vella, A. Ajdari, A. Vaziri, A. Boudaoud, Wrinkling551
 519 of pressurized elastic shells, *Physical Review Letters* 107552
 520 (2011) 174301.
- 521 [10] M. Taffetani, D. Vella, Regimes of wrinkling in pres-
 522 surized elastic shells, *Philosophical Transactions of the*
 Royal Society A: Mathematical, Physical and Engineer-
 ing Sciences 375 (2017) 20160330.
- [11] W. J. Stronge, *Impact mechanics*, Cambridge university
 press, 2018.
- [12] R. Cross, Dynamic properties of tennis balls, *Sports*
Engineering 2 (1999) 23–34.
- [13] J. Katz, Thump, ring: the sound of a bouncing ball,
European journal of physics 31 (2010) 849.
- [14] A. Georgallas, G. Landry, The coefficient of restitution of
 pressurized balls: a mechanistic model, *Canadian Jour-
 nal of Physics* 94 (2015) 42–46.
- [15] L. Tadrist, B. D. Texier, F. Lanzetta, L. Tadrist, Impact
 of a pressurised membrane: contact time, *International*
Journal of Impact Engineering 156 (2021) 103963.
- [16] Q. Guo, F. Zaïri, H. Baraket, M. Chaabane, X. Guo,
 Pre-stretch dependency of the cyclic dissipation in
 carbon-filled sbr, *European Polymer Journal* 96 (2017)
 145–158. URL: [https://www.sciencedirect.com/
 science/article/pii/S0014305717308674](https://www.sciencedirect.com/science/article/pii/S0014305717308674). doi:doi:
<https://doi.org/10.1016/j.eurpolymj.2017.07.015>.
- [17] L. Pauchard, S. Rica, Contact and compression of elastic
 spherical shells: the physics of a ping-pong ball, *Philo-
 sophical Magazine B* 78 (1998) 225–233.
- [18] R. Cross, Impact behavior of hollow balls, *American*
Journal of Physics 82 (2014) 189–195.
- [19] H. Feshbach, P. M. Morse, M. Michio, *Methods of theo-
 retical physics*, Dover Publications, 2019.
- [20] A.-L. Biance, F. Chevy, C. Clanet, G. Lagubeau,
 D. Quéré, On the elasticity of an inertial liquid shock,
Journal of Fluid Mechanics 554 (2006) 47–66.